Author manuscript of article in *Bioconjugate Chemistry* 2024, DOI: 10.1021/acs.bioconjchem.4c00412

# Dual responsive emulsions based on amphiphilic elastin-like polypeptide bioconjugates

*Laurianne Simon,[1,□,*] Dongxu Zhou,[2,□] Anita Coeurvolan,[1] Vincent Lapinte,[1] Sébastien Lecommandoux,[2] Elisabeth Garanger,[2,*] and Sylvie Bégu[1,*]*

[1] ICGM, Univ. Montpellier, CNRS, ENSCM, Montpellier, France
[2] Université de Bordeaux, CNRS, Bordeaux INP, LCPO, UMR 5629, ENSMAC, 16 avenue Pey-Berland, Pessac F-33600, France

□ co-first authors

Laurianne.simon@umontpellier.fr
Elisabeth.garanger@u-bordeaux.fr
Sylvie.begu@umontpellier.fr

## Abstract

To achieve the desired therapeutic response, drug delivery systems must ensure the controlled release of its loaded content at the targeted site. One possible strategy relies on the improvement of conventional drug delivery systems. To do so, smart polymers, able to change their behavior upon chemical, physical or biological stimuli, can be used. In this context, this study aims to evaluate the potential of a natural amphiphilic smart elastin-like polypeptides grafted with alkyl chains (ELP-*g*-Bu) to stabilize conventional oil in water emulsions and trigger the release of loaded molecules upon dual stimuli. With butyl pendant chains and methionine residues, the macromolecular surfactant ELP-*g*-Bu demonstrated a modification of physico-chemical properties, looking at critical aggregation concentration, upon both temperature and oxidation stimuli. The macromolecular surfactant was then able to stabilize a paraffin oil in water emulsion. The ELP-*g*-Bu emulsion presented a droplet size of 9 ± 1 µm and stability for at least a month at 4 and 25 °C. After a successful loading of fluorescent lipophilic molecule used as drug model, a complete destabilization of the ELP-*g*-Bu emulsion and burst release of the content was achieved with thermal triggering at 42 °C. In oxidative conditions, a partial release was measured which can be improved by increasing the number of oxidable thioether groups. Overall, these dually-responsive amphiphilic ELP-*g*-Bu demonstrated its potential for smart polymer-based drug delivery systems that can be promising for inflammatory diseases treatment as increased temperature and radical oxygen species are present in such cases.

**Keywords:** smart delivery system, thermal and ROS responsivity, demulsification, controlled release

**Graphical abstract**

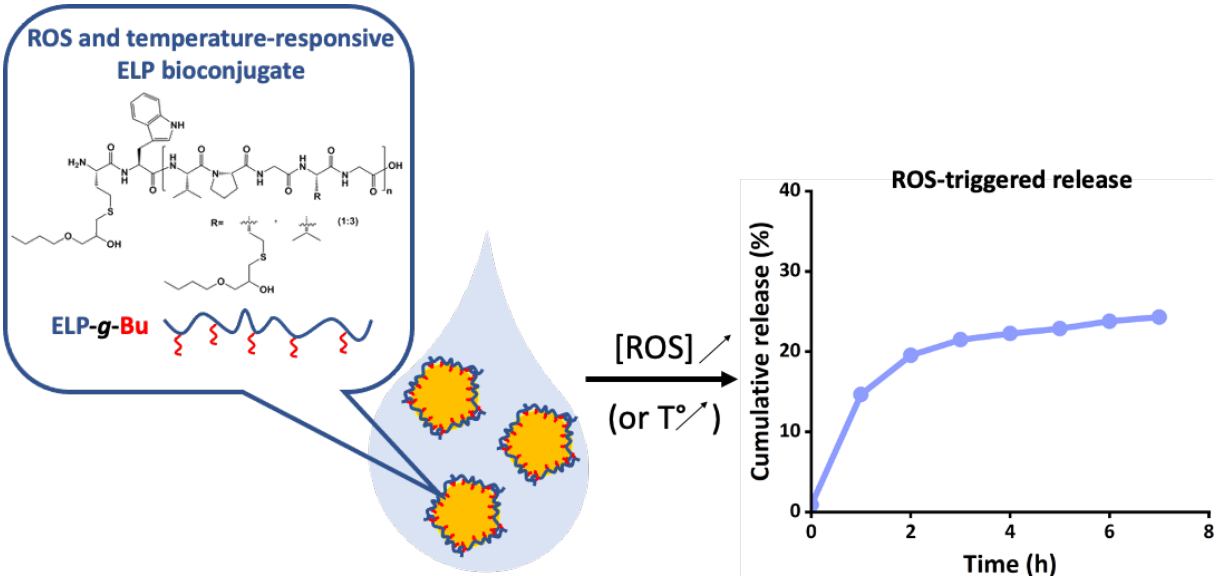

## 1. Introduction

Emulsions are amongst the most commonly used formulations in a wide variety of applications such as for food[1], pharmaceutics[2], or cosmetics[3]. Composed of two immiscible phases dispersed and stabilized by surfactant as emulsifier, they can encapsulate and protect hydrophobic or hydrophilic molecules with respectively oil-in-water (O/W) and water-in-oil (W/O) emulsions, with excellent control over droplets' size and size distributions[2]. The amphiphilic surfactant plays a key role for the emulsion stability through surface activity and structure formation at the interface between the two phases[3]. Moreover, the surfactant can be engineered to provide emulsions with controlled release properties of the loaded active molecule(s). For instance, properly designed smart polymers are able to trigger molecule release upon various external stimuli[4–6]. In fact, changes in the physico-chemical properties of surfactants upon specific stimuli, can strongly impact related properties such as surface activity, polarity or solubility. Therefore, in emulsions, these drastic modifications can trigger interactions between droplets and lead to droplets' destabilization and demulsification causing drug release[7]. A wide variety of stimuli have been explored. They mostly fit into three main categories *i*) physical stimuli such as temperature, light, magnetic or electrical fields[8], *ii*) chemical stimuli such as pH, $CO_2$ content, salt, radical oxygen species (ROS), and *iii*) biological stimuli with enzymes/receptors, antigens, ligands or biomolecules[9]. Combinations of different stimuli have also been reported. For instance, dually responsive emulsions based on smart polymers that can respond to two different stimuli have been described to trigger drug release[9]. For example, Dong *et al.* combined pH and UV blue light stimuli to trigger morphological change of a double emulsion of heptane/perfluorohexane/water thanks to the surfactant 1-[2-(4-decylazobenzene-phenoxy)-ethyl]-1-diethylenetriamine. Indeed, the addition of HCl induced the protonation of the amine group and UV irradiation the azobenzene group change from trans to cis state; causing in both cases the destabilisation[10].

Overall, two main family of stimuli-responsive polymers for emulsion applications have been described in the literature[7], either based on natural biopolymers (such as proteins or nucleic acids) that can be isolated and chemically modified, or purely synthetic ones containing appropriate functional groups responding to the stimuli. Among bioinspired smart polymers, elastin-like polypeptides, also called ELPs, are intrinsically disordered recombinant protein polymers, constituted of repeating [-Val-Pro-Gly-*Xaa*-Gly-] pentapeptide units (*i.e.*, -VPGXG-)[11]. ELPs possess several advantageous properties such as biocompatibility, biodegradability, non-immunogenicity and are thermally responsive[12]. Indeed, they present a reversible soluble-to-insoluble phase transition with a lower critical solution temperature (LCST) behavior. The latter allows their isolation and non-chromatographic purification from bacterial lysates,[13,14] and additionally provides a means to trigger their reversible self-assembly in aqueous conditions upon the application of external stimuli (*e.g.*, local temperature, addition of co-solutes)[15]. Therefore, ELPs are highly attractive biopolymers for biomedical applications such as drug delivery with ELP-drug conjugates, hydrogels or nanoparticles[16–19]. More especially, properly designed ELPs

can self-assemble into micelles[20] or vesicles[21–23], and be exploited as biocompatible drug nanocarriers[24,25], as well as bioactive nano-objects[26–28]. However, molecular and bacterial cloning steps can be long and tedious, somehow limiting the rapid access to a large variety of ELPs with different macromolecular characteristics. Therefore, one strategy to overcome these issues relies on a dual biotechnological and chemical approach consisting in the engineering of recombinant ELP scaffolds and in their subsequent post-modifications by synthetic bioorthogonal reactions to readily access a wide variety of ELP-based bioconjugates. In particular, a library of recombinant ELPs containing regularly spaced methionine as guest residue (X) in (VPGXG) repeat units was engineered (ELP[$M_1V_3$-n], n=20-100) in our group[29], and chemoselective alkylation reactions at the thioether group of methionine were applied[30,31] to access various ELP bioconjugates (*e.g.*, glycopolypeptides[32,33], lipopolypeptides[21], cationic polypeptides[34,35]) for different applications. Chemical oxidation of methionine thioether group was also evidenced to have a major impact on the physico-chemical properties of a designed ELP[34]. While native methionine residues confer a hydrophobic character to an ELP chain (low cloud point temperature, $T_{cp}$), oxidation of the thioether group into sulfoxide drastically increases the hydrophilicity of the polypeptide and therefore leads to a high $T_{cp}$[36]. In a previous study, our group has taken advantage of this property to design a ROS-responsive ELP bioconjugate[37] allowing the disassembly of micellar coacervates at 37 °C into individual micelles upon light irradiation and ROS generation.

In the present study, the potential of a dually-responsive amphiphilic ELP to stabilize emulsions and control the release of loaded molecules upon external stimuli was evaluated. To this aim, a new ELP derivative was synthesized from the ELP[$M_1V_3$-80] scaffold grafted with butyl pendant chains at the side chain of all methionine residues (ELP-*g*-Bu) to obtain surfactant properties. In particular, the critical aggregation concentration (CAC) of ELP-*g*-Bu was determined in different media and different temperature conditions. The impact of thioether groups' oxidation onto physico-chemical properties was also evaluated to anticipate the potency of an oxidative stimulus to destabilize ELP-*g*-Bu-based O/W emulsions. After a screening of the emulsion composition ratio and process parameters, the selected ELP-*g*-Bu stabilized emulsion was studied for the triggered release of loaded molecules upon heating at physio-pathological temperature and ROS-mediated oxidation of the macromolecular surfactant.

# 2. Materials and Methods

## 1. Materials

Butyl glycidyl ether (TCI, 98 %) and ammonium 1-pyrrolidinedithiocarbamate (APDC, Acros Organics, 98 %) were used as received. Glacial acetic acid (AcOH, Sigma-Aldrich, 99 %), hexafluoroisopropanol (HFIP, abcr, 99%), methanol (MeOH, VWR chemicals), ethanol (EtOH, VWR chemicals) and acetonitrile (Fisher Scientific, 99.8 %) were used as received without additional purification. Ultrapure water (18.2 MΩ·cm$^{-1}$) was prepared using a Millipore Milli-Q system. Amicon Ultra-15 Centrifugal filter tubes were used for the purification of ELP derivatives. Phosphate Buffer Saline (PBS) tablets at 150 mM were purchased from Sigma (Saint-Louis, USA) and provide, upon appropriate solubilization, 137 mM sodium chloride NaCl, 2.7 mM potassium chloride KCl and 10 mM phosphate buffer solution (pH= 7.4). Hydrogen peroxide (30 % $H_2O_2$ in water), liquid paraffin, paraffin oil, Nile red and fluorescein isothiocyanate (FITC) were purchased from Sigma Aldrich (Saint-Louis, USA). Dialysis tubbings were obtained from Spectrum Labs (San Francisco, USA). Microscope slides and cover slides were respectively purchased from Labsolute (Braunschweig, Germany) and Knittel glass (Renningen, Germany).

ELP[$M_1V_3$-80] (Figure 1A) was produced recombinantly in *Escherichia coli* and isolated by inverse transition cycling following previously reported procedures[29].

## 2. Methods

### Elastin-like polypeptide derivatives synthesis

**Synthesis of ELP-*g*-Bu($S^+$)**

The synthesis of the ELP-*g*-Bu($S^+$) intermediate was performed adapting a previously published procedure (Figure 1B)[30]. ELP[$M_1V_3$-80] (1 equiv.) was dissolved in AcOH/HFIP (9:1) mixture at a concentration of 10 mg/mL and flushed with argon for 20 min. Then butyl glycidyl ether (10 equiv./Met, *i.e.*, 210 equiv.) was added. The reaction was left at room temperature for 48 hours and most of the solvent was evaporated under vacuum to get a viscous solution. The latter was diluted with cold water and then transferred to centrifugal filter tubes which were previously washed with 10 % EtOH aqueous solution. The solution was washed with water for several centrifugation cycles and finally lyophilized to obtain ELP-*g*-Bu($S^+$) as a white solid. Yield > 75 %. The compound was analyzed by $^1$H NMR (400 MHz, $D_2O$) and SEC (Figure S1) with the following attribution $^1$H NMR ($D_2O$, 400 MHz): δ(ppm) = 4.50–4.37 (m, 160 H, CHα Val and Pro, VPGXG), 4.23-4.14 (m, 80.5 H, CHα Val, VPGVG and -CH-(OH)), 3.06-2.93 (m, 61.5 H, $S^+$-$CH_3$), 1.64-1.51 (p, 41 H, -O-($CH_2$)-$CH_2$-), 1.41-1.29 (h, 41 H, -O-($C_2H_4$)-$CH_2$-).

**Synthesis of ELP-*g*-Bu**

The demethylation of ELP-*g*-Bu($S^+$) was achieved following a previously reported procedure (Figure 1B)[30]. In brief, ELP-*g*-Bu($S^+$) (1 equiv.) was dissolved in 75 % (v/v) EtOH aqueous solution at a concentration of 10 mg/mL and flushed with argon for 20 min. Then, APDC (5 equiv./Met, *i.e.*, 105 equiv.) was added and the reaction was stirred at room temperature for 24 hours. The reaction mixture was then transferred into dialysis tubbings (MWCO = 1 kDa) and dialyzed first against 50 % MeOH (aq.) for 24 hours and then against ultrapure water for 24 hours with three changes of each solvent. Finally, the solution was lyophilized to obtain ELP-*g*-Bu as a white powder. Yield > 65 %. The compound was analyzed by $^1$H NMR (400 MHz, $D_2O$) and SEC (Figure S1).

**Synthesis of the control compound ELP-*g*-Bu(SO)**

ELP-*g*-Bu was dissolved in 30 % $H_2O_2$ in aqueous solution at 0 °C for 30 min in order to oxidize the thioether groups into sulfoxide. Few drops of 1 M sodium thiosulfate aqueous solution were then added to the solution to quench the reaction before transferring into dialysis tubbing (MWCO = 3.5 kDa). The solution was dialyzed against ultrapure water for 48 hours with two changes of water per day. The solution was then lyophilized to obtain ELP-*g*-Bu(SO) as a powder. $^1$H NMR (400 MHz, $D_2O$) analysis was performed to confirm oxidation and determine the percentage of ELP oxidation (Figure S2).

ELP-*g*-Bu(SO) intermediates with various degrees of oxidation were also synthesized by tuning the amount of $H_2O_2$. These were analyzed by $^1$H NMR (400 MHz, $D_2O$) (Figure S2). Firstly, the resonance peak at 4.2 ppm was used for calibration (integral set at 160). The degree of oxidation of each intermediate was then determined by calculating the ratio of the integral (AUC) of the shifted resonance peaks of interest at 3.0-2.7 ppm (*l'*, *t'*) of the oxidized species and the AUC of the peaks at 2.5-2.3 ppm (*l*, *t*) for the non-oxidized compound (ELP-*g*-Bu, AUC of 82).

## $^1$H NMR spectroscopy

$^1$H NMR spectra were recorded with a Bruker AVANCE III HD equipment (Liquid-state 400 MHz NMR spectrometer with 5 mm BBFO probe). Deuterated water ($D_2O$, Euriso-top, 99.9 %) was used as solvent.

## Size exclusion chromatography

Samples were analyzed on an Ultimate 3000 system from Thermo Scientific equipped with a diode array detector (DAD). The system also includes a multi angle light scattering detector (MALS) and a differential refractive index detector (dRI) from Wyatt Technology. Samples were separated on one TSK G3000HHR (7.8*300) column and one TSK G2000HHR (7.8*300) column. Analyses were performed at a flow rate of 0.5 mL·min$^{-1}$ and dextran was used as standard.

## Critical aggregation concentration determination by Nile Red and pendant drop method

The determination of the critical aggregation concentration (CAC) was first conducted using the Nile red fluorescence probe. To measure the CAC values of the different ELP derivatives, their solution in

water and PBS at different concentrations were firstly prepared. Then, 1 µL of 0.1 mg/mL Nile red solution in acetonitrile was added to 500 µL of ELP derivative solution, leading to a final concentration of Nile red was 0.2 µg/mL. All samples were then subjected to fluorescence measurements upon a temperature ramp from 4 to 50 °C with an interval of 2 °C. The CAC was defined as the concentration at which an abrupt increase of fluorescence intensity was observed. (Figure S3)

Fluorescence measurements were carried out on a JASCO FP-8500 fluorescence spectrometer equipped with a JACOB MCB-100 circulation bath. All measurements were performed using a quartz cell with a light path of 3×3 mm at different temperatures. To obtain the emission spectra and determine the maximum emission wavelength ($\lambda_{em}$), the excitation wavelength was fixed at 500 nm and an emission wavelength range of 550-750 nm was applied. To measure the fluorescence intensity of different samples, the excitation wavelength was fixed at 500 nm and the emission wavelength was fixed at the maximum $\lambda_{em}$ for each sample.

The CAC values for ELP derivatives were also measured by the pendant drop method. To do so, the drop shape analyzer KRÜSS DSA100 equipped with a CF04 camera (160 fps at 1200 × 1200 px) and a needle with a diameter of 1.83 mm was used to measure the surface tension of sample droplets exposed to air. The equipment is placed in a clean room (ISO 7) with a humidity atmosphere around 55 % (+/- 10 %) and an overpressure of 60 Pa. Solutions of the different ELP derivatives at different concentrations in water and PBS were firstly prepared. One drop of each sample was made and the surface tension was measured at one fixed temperature of 22 °C. The CAC value was defined as the end point of the linear decay of surface tension.

## Determination of cloud point temperatures by nephelometry

The cloud temperature ($T_{cp}$) of ELP derivatives was determined by nephelometric measurement on spectrofluorophotometer RF-6000 (Shimadzu, Japan) equipped with a temperature controller cell holder (Quantum northwest, USA). Measurements were determined by using 5 nm slit widths at an excitation wavelength of 520 nm. Data were collected on Labsolution software. ELP-*g*-Bu($S^+$) and ELP-*g*-Bu derivatives were analyzed at a concentration of 16.6 µM below the CAC in ultrapure water and in PBS solutions. Quartz cuvettes were filled with ELP derivatives solutions and a temperature ramp from 10 °C to 80 °C at a heating and cooling rate of 2 °C/min was applied.

## Formulation of ELP-*g*-Bu based emulsions and characterization

The emulsion composition and process parameters were determined by conducting a pre-formulation study with a ternary diagram elaboration. To do so, the emulsion composition was screened with a fixed weight ratio of ELP-*g*-Bu of 10 % and a gradual increase of oil weight ratio. Thus, the ratio ELP-*g*-Bu:Paraffin oil:Water ranging from 10:30:60 to 10:10:80 was tested. The emulsions were performed using ultrasonic probe Sonifier 250 (Branson, USA) designed to work on small volume (0.1 mL to 10 mL). ELP-*g*-Bu was placed under magnetic stirring for 48 hours in the ultrapure water in sealed vials.

Paraffin oil was added into the tube previously placed in a cold bath. The ultrasonic probe was then immerged into the emulsion with different parameters (duty cycle, time and control output).

Non-diluted emulsions were observed using the optical microscope EVOS M5000 (Invitrogen, USA) with magnification ×10 and ×40. Then, pictures were processed with Image J software to determine the mean diameter of droplets (minimum of 30 pictures taken for each sample).

## ELP-*g*-Bu based emulsion stability study

A stability study was carried out by placing three batches of emulsions at different conditions (4 °C and 25 °C). The emulsion stability was monitored every seven days (D7, D14, D21 and D28, n=3) with observation under optical microscope EVOS M5000 (Invitrogen, USA).

## Emulsions loading and selective release

ELP-*g*-Bu emulsions were loaded with Nile red to investigate their thermo-responsive properties. After dissolving Nile red in paraffin oil at 2 mg/mL, this oil mixture was added to emulsions according to the selected ratio. The emulsion fluorescence intensity was measured before (20 °C) and after the $T_{cp}$ (42 °C) previously determined by nephelometry.

Emulsions were loaded with fluorescein isothiocyanate (FITC) at 2 mg/mL and placed into dialysis tubbing (MWCO = 3.5 kDa). Dialysis was performed against a solution of hydrogen peroxide (30 % w/w in water) under agitation for 8 hours. Every hour, 1 mL sample of medium was analyzed by fluorophotometer RF-6000 (Shimadzu, Japan) and replaced by 1 mL of fresh medium to maintain a constant volume. Fluorescence intensity values were collected using Labsolution software. The release percentage was calculated with the fluorescence measured at each time point compared to the fluorescence of full release. The 100 % release was determined with the fluorescence quantification of the emulsion directly added to the 30 % $H_2O_2$ medium.

# 3. Results and discussion

## 1. Synthesis of the amphiphilic ELP-*g*-Butyl (ELP-*g*-Bu) bioconjugate

ELP-*g*-Bu was synthesized in two steps from the recombinant ELP[$M_1V_3$-80] containing a total of 21 methionine residues, thereafter noted as ELP (Figure 1A). The ELP was first thioalkylated using butyl glycidyl ether to yield ELP-*g*-Bu($S^+$) which was subsequently demethylated using the ammonium 1-pyrrolidinedithiocarbamate (APDC) (Figure 1B). ELP, ELP-*g*-Bu($S^+$) and ELP-*g*-Bu derivatives were analyzed by SEC and $^1$H NMR spectroscopy (Figure S1). SEC chromatograms were in good agreement with previous observations[31]. Due to the positively charged sulfonium groups and associated counter anions that can interact with the columns, ELP-*g*-Bu($S^+$) has a longer elution time despite a higher molar mass as compared to ELP (as already observed with a similar ELP-based lipopolypeptide)[21] (Figure S1B), while the demethylated ELP-*g*-Bu has a shorter elution time in agreement with its higher molar mass and hydrodynamic volume as compared to the pristine ELP. The $^1$H NMR spectra of all derivatives in $D_2O$ were also in agreement with the expected chemical structures (Figure S1C). Compared to the sample before demethylation (ELP-*g*-Bu($S^+$), blue trace), the resonance peaks of protons *m* and of acetate anions disappeared in the spectrum of ELP-*g*-Bu (red trace) confirming the complete demethylation of ELP-*g*-Bu($S^+$). According to the $^1$H NMR analysis, the average conversion rate was found around 97% (*i.e.*, 20.5 methionine residues are grafted with butyl chains over a total of 21).

The gradual oxidation of ELP-*g*-Bu was achieved in order to evaluate the impact of thioether groups' oxidation onto the CAC values. The compound, ELP-*g*-Bu(SO) (Figure 1C), with all thioether groups oxidized into sulfoxides was also synthesized as control. The conversion of thioether groups into sulfoxide was monitored by $^1$H NMR analysis in $D_2O$ (400 MHz) and compared with non-oxidized ELP-*g*-Bu (Figure S2). The resonance for protons *l* and *t* on the side chain at $\delta$ = 2.5-2.3 ppm was shifted to 3.0-2.7 ppm (*l'* and *t'*) in ELP-*g*-Bu(SO). The calculation of oxidation degrees was based on the ratio of AUC *l', t'*/82 as detailed in supplementary data (Table S1). Similarly, the relation between the percentage of thioether groups' oxidation versus the amount of $H_2O_2$ was plotted (Table S1). Interestingly, a linear correlation can be drawn between the percentage of oxidation and the logarithm of the ratio of $H_2O_2$ to ELP used.

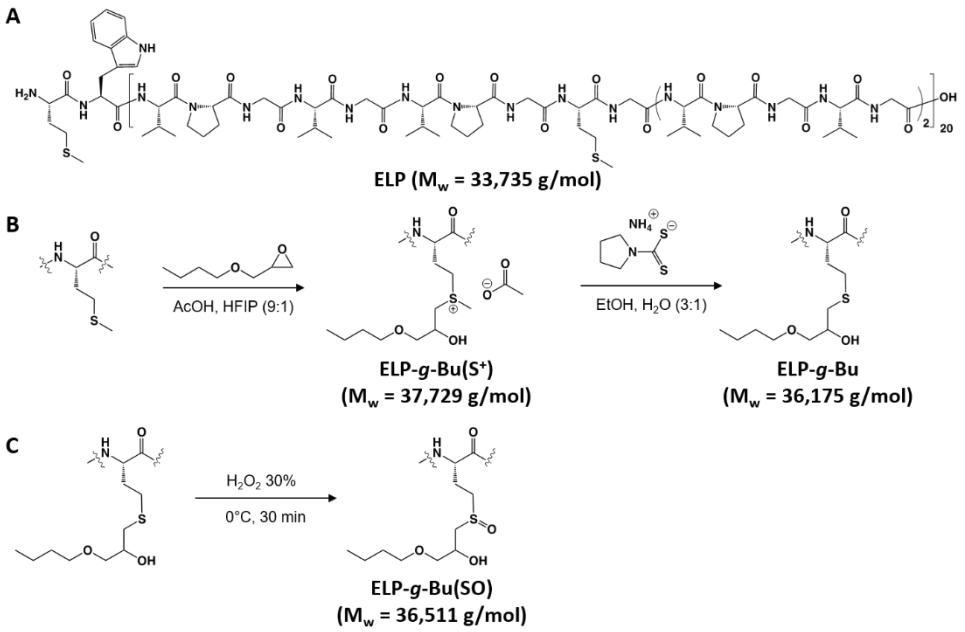


Figure 1. A) Chemical structure of ELP[$M_1V_3$-80], simplified as ELP. Simplified synthetic schemes to access B) ELP-*g*-Bu($S^+$), ELP-*g*-Bu, and C) ELP-*g*-Bu(SO) derivatives. The molar masses ($M_w$) of all compounds are also provided.

## 2. Physico-chemical characterizations of ELP derivatives grafted with butyl chains

Before exploring the capacity of ELP-*g*-Bu to stabilize O/W emulsions, physico-chemical properties, namely the CAC and thermal responsiveness, of the different derivatives synthesized were studied. The CAC of both ELP-*g*-Bu($S^+$) and ELP-*g*-Bu was measured by fluorescence spectroscopy using Nile red as fluorescent probe and by the pendant drop technique (Table S2). As illustrated on Figure 2A, the CAC of ELP-*g*-Bu($S^+$) in water was independent of temperature in the temperature range studied (4-50 °C) and found around 1.76 mg/mL (46.65 µM). This result is consistent with the hydrophilic character of sulfonium groups present all along the polypeptide chain that significantly increase the hydrophilicity, as already demonstrated[30,31]. The demethylation of ELP-*g*-Bu($S^+$) however strongly affected the CAC of the resulting ELP-*g*-Bu as reflected by the significant decrease of the CAC value from 1.76 mg/mL at 22 °C for ELP-*g*-Bu($S^+$) to 0.062 mg/mL for ELP-*g*-Bu (Figure 2B and 2C). The CAC of ELP-*g*-Bu was slightly affected by temperature (Figure 2 B) with a value ranging from 0.061 mg/mL (1.7 µM) at 4 °C to 0.046 mg/mL (1.29 µM) at 50 °C. These results were consistent with the recovery of a thioether group (more hydrophobic than a sulfonium group) upon the demethylation reaction[30].

The impact of salts on CAC was also monitored with measurement carried out in PBS at 150 mM to mimic physiological conditions. The CAC of ELP-*g*-Bu($S^+$) in PBS (1.53 mg/mL at 22 °C) was found slightly lower than in water, and independent of temperature similarly to what was observed in water (Figure S4A). However, the CAC of ELP-*g*-Bu was strongly affected by the presence of salts especially after reaching the temperature of 28 °C (Figure S4B). Indeed, from 4 °C to 28 °C the CAC value

remained constant around 0.08 mg/mL (2.3 µM) which is close to the value in water. However, a faint but continuous decrease of the CAC was observed upon increasing temperature from 30 °C (0.06 mg/mL, 1.6 µM) to 50 °C (0.026 mg/mL, 0.72 µM). The control of temperature and salinity was therefore found to be a prerequisite for our subsequent emulsification study. Similar results were obtained with the pendent drop method thus confirming the robustness of the CAC determination (Figure S5 and Table S2). With this method, the effectiveness (ΔST) was also determined to reflect the ELP derivatives' ability to reduce the surface tension (Table S2). The demethylated ELP-*g*-Bu showed high effectiveness with 22.5 ± 0.4 mN/m in water and 25.2 ± 0.2 mN/m in PBS, while the effectiveness of the positively charged ELP-*g*-Bu($S^+$) derivative was measured at 19.4 ± 0.2 mN/m and 21.0 ± 0.2 mN/m respectively. The ELP-*g*-Bu derivative therefore consistently demonstrated higher surfactant capacity than the more hydrophilic ELP-*g*-Bu($S^+$) derivative.

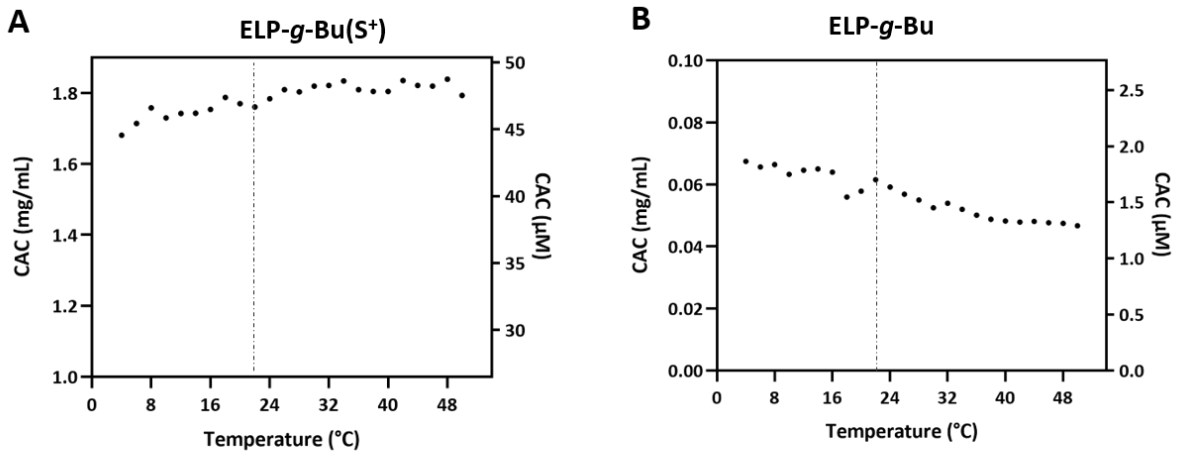


C

| 22°C | CAC (mg/mL) | CAC (µM) |
|---|---|---|
| ELP-*g*-Bu($S^+$) | 1.76 | 46.65 |
| ELP-*g*-Bu | 0.062 | 1.70 |

Figure 2. Determination of the critical aggregation concentration (CAC) in mass concentration (mg/mL) and molar concentration (µM) using Nile red as fluorescent probe in water with increasing temperature of A) ELP-*g*-Bu($S^+$) and B) ELP-*g*-Bu**.** C) CAC values at 22 °C for the two ELP derivatives in water.

The effect of oxidation of thioether groups of ELP-*g*-Bu on CAC values was also investigated to anticipate the potential behavior changes to ROS exposure. To do so, the ELP-*g*-Bu derivative was oxidized at gradual degree from 0, 20, 42, 88 to 100 %. Quantification by $^1$H NMR spectroscopy was used to determine the degree of oxidation of thioether groups into sulfoxide (Figure S2). The CAC of the different derivatives was determined at 22 °C in water using the Nile red method and expressed in mass concentration (black dots) and molar concentration (red dots) (Figure 3). As the oxidation degree increased, the CAC value gradually increased as well from 0.062 mg/mL (1.70 µM) of ELP-*g*-Bu to 0.55 mg/mL (15.1 µM) for the fully oxidized compound ELP-*g*-Bu(SO). These results were confirmed with the pendant drop method (Table S3). The effectiveness represented as ΔST in Table S3 showed

however that before and after oxidation the ability of ELP to decrease surface tension remained overall constant. The gradual increase of CAC upon oxidization reflected the structural changes resulting in the increase of hydrophilicity. A change of behavior with ROS exposure and oxidation of methionine residues' thioether group is therefore expected.

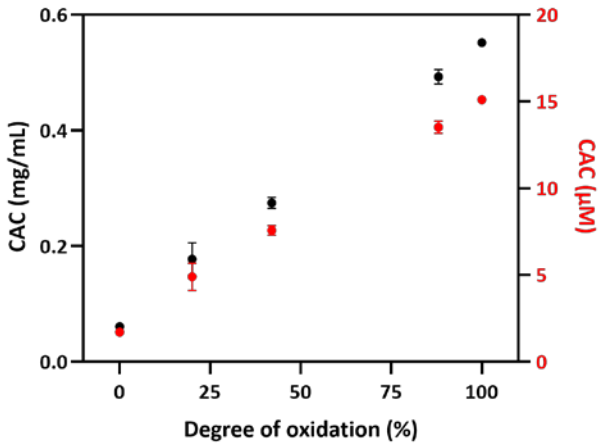


Figure 3. Determination of the CAC in water of ELP-*g*-Bu(SO) in mass concentration (mg/mL) in black and molar concentration (µM) in red upon oxidation degree from 0 to 100 % at 22 °C using Nile red as fluorescent probe.

The thermal responsiveness of ELP derivatives was also further characterized by measuring the cloud point temperature ($T_{cp}$) of the different derivatives. Nephelometry was used to estimate the $T_{cp}$ since more sensitive than UV-Vis spectroscopy or turbidimetry. An increase of scattered light intensity (SI) was identified as the onset of phase transition corresponding to the $T_{cp}$. (Figure S6) The effect of the temperature to induce the aggregation of the different derivatives (ELP-*g*-Bu($S^+$), ELP-*g*-Bu and ELP-*g*-Bu(SO)) at 17 µM in aqueous solution was evaluated in water and PBS. First of all, all ELP derivatives displayed thermal responsiveness but each polymer displayed a different $T_{cp}$ due to their different chemical structures. As expected, the positively charged ELP-*g*-Bu($S^+$) displayed a higher $T_{cp}$ (36 °C) as compared to the more hydrophobic demethylated ELP-*g*-Bu (22 °C). Similarly, the oxidation of thioether groups into sulfoxides induced higher $T_{cp}$ to 34 °C with ELP-*g*-Bu(SO) as compared to ELP-*g*-Bu at 22 °C. Indeed, ELP-*g*-Bu(SO) became more hydrophilic resulting in a better solubility in water[18]. These results were consistent with previous findings by Dai *et al.* , who studied the series of ELP[$M_1V_{3-n}$] ELP20, 40 and 60 and noticed the consequence of dependency between $T_{cp}$ and the hydrophilic diblock behavior as their ELP $T_{cp}$ moved from a range from 20-35 °C to 30-55 °C after oxidation[29].

Lastly, the influence of salts, with measurements conducted in PBS, was investigated and for each ELP derivative the $T_{cp}$ was reduced by 4 to 6 °C as compared to the ones in water. The shift of $T_{cp}$ in the presence of salts has been widely reported using the Homfeister series. In fact, the addition of kosmotropic anions (here NaCl) triggers the aggregation temperature of ELP by lowering the $T_{cp}$. Those

anions display a salting out effect causing a polarity increase by forming hydration complexes with water and get excluded from the polymer surface region[38–41]. Consequently, the cloud point temperature was affected by the structural changes in ELP such as demethylation and oxidation while maintaining thermo-responsiveness. Overall, the three ELP derivatives showed CAC values, ability to lower surface tension and thermo-responsiveness. ELP-*g*-Bu was selected for the emulsion formulation as its CAC value was lower in water and PBS and showed significant behavior changes upon heating and oxidation thus a promising candidate as smart polymer to stabilize O/W emulsions and trigger the release of loaded molecules upon these two stimuli.

## 3. Formulation of ELP-*g*-Bu based emulsions for selective drug release

Smart ELP-*g*-Bu macromolecular surfactant was thus used to stabilize conventional emulsions as a model system for the proof of concept of stimuli-triggered selective release. The response of the ELP-*g*-Bu based emulsion to external stimuli such as oxidation *via* ROS addition or temperature change was then further evaluated.

### Pre-formulation of ELP-*g*-Butyl emulsions

From the literature, most of the studies conducted on responsive emulsions used synthetic oils like silicone[42], paraffin[43] or n-decane[44]. As a first proof of concept, the oil selected for the formulation was the easily emulsifiable mineral paraffin oil. Aiming towards a stable emulsion with the highest possible oil percentage, a ternary diagram was established to determine the emulsion composition with a fixed weight ratio of ELP-*g*-Bu of 10 % w/w and a gradual increase of oil weight ratio (Figure 4 A). Considering its high hydrophilic-lipophilic balance (using Griffin method HLB = 18.6), ELP-*g*-Bu was mixed in water as it is more hydrophilic and to ensure the role of surfactant. After optimizing parameters of the ultrasonication step and weight ratios, emulsions of two size ranges were distinguished. Emulsion droplets above 50 µm were obtained with a ratio surfactant:oil:water (S:O:W) of 10:30:60. Smaller sized droplets (under 15 µm) were obtained with a ratio from 10:10:80 to 10:18:72 as illustrated Figure 4 A. After a centrifugation stability test, the emulsion composition was selected with a weight ratio S:O:W of 10:10:80 for its higher stability and smaller size which was not the case for emulsion 3 and 4 in the table of Figure 4 B. Then, process parameters were optimized by decreasing sonication time from 60 seconds to 45 seconds helping to reduce droplets' size. Therefore, the final emulsions presented a mean size of 10 ± 3 µm and the oil-in-water dispersion was confirmed by a coloring test with methylene blue and sudan red dyes (data not shown).

A

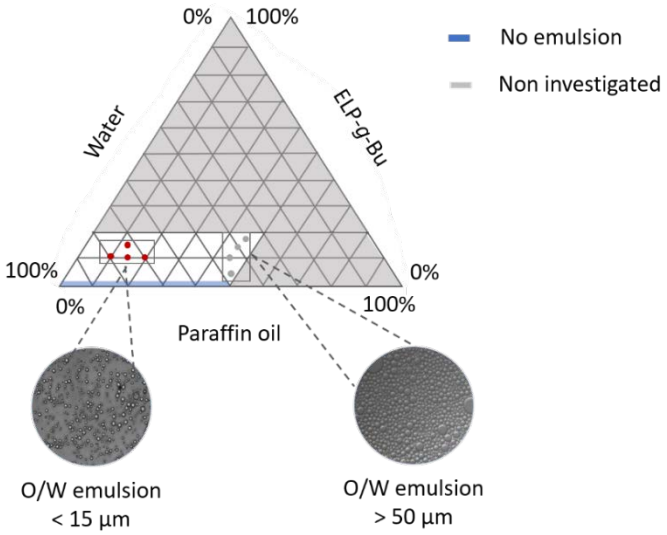


B

| ELP-*g*-Bu Emulsion | 1 | 2 | 3 | 4 |
|---|---|---|---|---|
| Duty cycle (%) / Output control time (s) | 40/2/**60** | 40/2/**45** | 40/2/**45** | 40/2/**45** |
| Weight ratio S:O:W | 10:10:80 | 10:10:80 | 10:**15**:75 | 10:**18**:72 |
| Size (µm) | 15 ± 2 | 10 ± 3 | 8 ± 2 | 9 ± 3 |

Figure 4. Screening of ELP-*g*-Bu based emulsion composition with A) ternary diagram elaboration and B) process parameters optimization with ELP-*g*-Bu emulsions < 15 µm (red dots in panel A).

The selected ELP-*g*-Bu based emulsion with a weight ratio (S:O:W) of 10:10:80 presented in Figure S7 was further characterized in Figure 5. The optical microscopy (Figure 5 A) revealed monodispersed paraffin oil droplets with a size distribution from 8 µm (8 %) to 18 µm (10 %) (Figure 5 B) and centered around 10 µm (27 %). Overall, the mean size of the selected emulsion was measured at 9 ± 1 µm and then a stability study was conducted to evaluate the impact of time and temperature on the emulsion size. As shown in the histogram in Figure 5 C, the size of the emulsion remained constant at 4 °C with a size of 10 ± 1 µm after 28 days. Similarly at 25 °C, the droplet size was not affected by the temperature with a size of 13 ± 2 µm reached after 28 days as illustrated in the microscope images in Figure S8. Similarly, this stability of emulsion stabilized with smart polymers was also observed with pH-responsive surfactant stabilizing a *n*-decane oil-in-water emulsion with stability over a month at a concentration above the CAC and average droplet diameter remaining around 30 µm[44]. The stability study was not conducted as above 25 °C as the thermo-responsiveness of the ELP-*g*-Bu generated its aggregation as shown in Figure S4. Indeed, as also observed by Feng *et al.*, with thermo-responsive surfactant stabilizing O/W emulsion with silicone oil, heating above the LCST led to emulsion breaking down with droplets collapsing quickly to form bigger droplets[42].

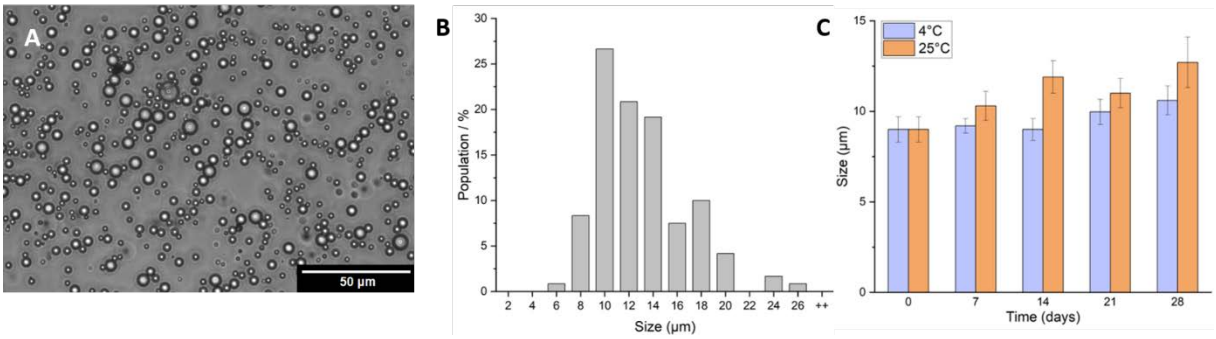


Figure 5. Selected ELP-*g*-Bu emulsion with S:O:W of 10:10:80 with A) optical microscopy observation, B) size distribution histogram (n=3), and C) stability study at 4 and 25 °C over a month (n=3).

## Cargo loading of ELP-*g*-Bu emulsions and release study upon temperature and oxidation stimuli

After verifying the stability of ELP-*g*-Bu based emulsions, the destabilization and release by applying temperature change and oxidation by ROS stimuli were investigated. First, to evaluate the thermo-responsive release, Nile red (hydrophobic fluorescent probe) was loaded and its release was measured by spectrofluorometry (Figure 6 A). At low temperature (20 °C), a bell curve was drawn as the intensity highly increased to peak at 130,000 A.U. around 640 nm. Increasing temperature to 42 °C for 30 minutes impacted the fluorescence intensity which crumbled and reached low values under 1,000 A.U. The significant drop in fluorescence intensity was a consequence of Nile red release from ELP-*g*-Bu emulsions. In fact, a temperature of 42 °C induced a change of behavior of ELP-*g*-Bu present at the oil-water interface by forming an aggregate due to the ELP phase transition behavior. Aggregation caused coalescence and, as a result, the incorporated Nile red was released from the droplets into the aqueous phase. Since Nile red has no fluorescence signal in water, the intensity decreased and reached low values as illustrated Figure 6 A.

Lastly, the response of ELP-*g*-Bu stabilized emulsions to oxidation with $H_2O_2$ used as ROS was investigated. To do so, fluorescein isothiocyanate (FITC) was loaded in the emulsion and its release was quantified using a spectrofluorometer (Figure 6 B). With the FITC loaded emulsion placed in a dialysis tubbing, the release was measured for 8 hours in 30% aqueous $H_2O_2$ medium punctually every hour. Although due to the limited quantity of ELP-*g*-Bu and $H_2O_2$ concentration of 30 %, only a maximum of 50 % oxidation rate of ELP-*g*-Bu(SO) was possible. Therefore, this experiment led to preliminary results regarding ROS triggered release (Figure 6 B). Progressive release over time was observed, with a plateau of 25% release reached after 8 hours. To ensure the measurement of the release was due to the oxidation of methionine groups only, a control in $H_2O$ was also conducted. Indeed, the release of the emulsion loaded with FITC and stabilized by ELP-*g*-Bu was studied in water at pH 3.2 (same pH as $H_2O_2$ solution) called control $H_2O$ (Figure 6 B). Eventually, the control of FITC loaded emulsions in water at pH 3 showed a leakage of FITC by itself of 8 %. This is explained by the amphiphilic nature of FITC which tend to go in the aqueous phase. Thus, considering the values of FITC leakage at a pH of 3.2, the release

triggered by the oxidation of the methionine groups was about 17 %. Therefore, the oxidation stimuli led to partial release of 17 % when 50 % of the ELP-*g*-Bu methionine groups were oxidized. To achieve full release, the structure of ELP-*g*-Bu could be modified to include more methionine groups so that such an emulsion can be of use for therapeutic application involving the triggering of oxygen radical species in an inflammatory state. To the best of our knowledge, none of the stimuli-responsive polymers conventional emulsions studied the release of loaded molecules upon external chemical stimuli.

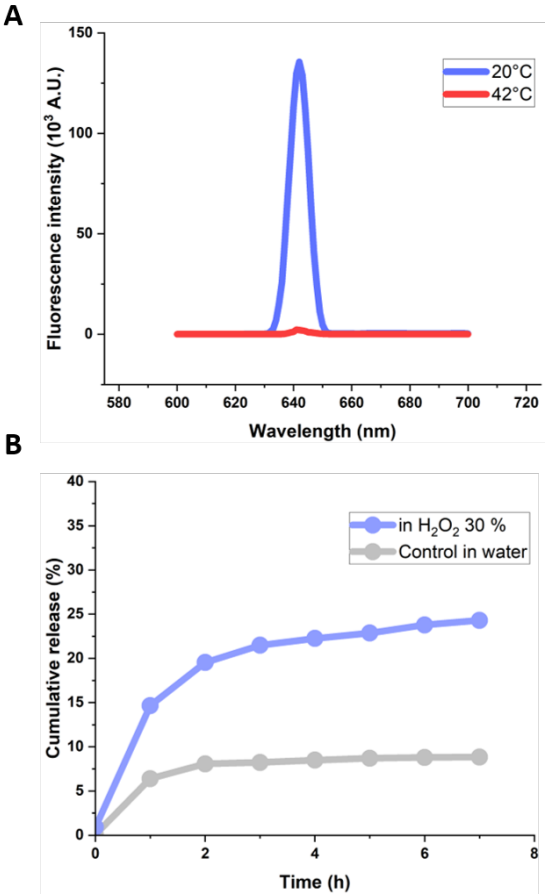


Figure 6. Destabilization and release of loaded molecules from ELP-*g*-Bu emulsion upon external stimuli with A) upon temperature stimulus with Nile Red loaded and B) upon oxidation stimulus with $H_2O_2$ solution at 30 % with FITC loaded.

Looking at the literature, most of the chemical stimuli-responsive emulsions are stabilized by solid particles known as Pickering emulsions. Responsive Pickering emulsions can be stabilized either by a polymer attached to a solid particle surface, by microgels of polymers or by hydrophilic particles stabilized with electrostatic interactions[9,45]. Focusing only on conventional engineered emulsions to compare with the one developed with ELP-*g*-Bu, thermo-responsive or pH-responsive emulsions are the most common chemical stimulated ones. The thermo-responsive emulsions usually relied on polymers with the LCST (usually above human physiological temperature) inducing the polymer shift from water soluble to insoluble creating a structure collapse such as with the work of Verbrugghe *et al.*, with PVCL-based graft copolymers[46]. On the contrary, some polymer solutions transform into a gel state with sol-

gel transition above critical temperature with PNIPAM-*co*-PEGMA graft enabling switching from liquid emulsion to a vicious gel[47,48]. This strategy was extensively used as described in a recent review on stimuli-responsive polymers for engineered emulsions[7]. Working with stimuli responsive emulsions stabilized by a biopolymer, the study of Tirgarian *et al.,* using kappa-carrageenan illustrated the pH-responsivity potential. Similarly, after the synthesis of the biopolymer and evaluation of the emulsifying properties, they formulated an O/W emulsion with soybean oil and loaded with sudan III red dye with a droplet size ranging from 5 to 2 µm. However, these emulsions displayed creaming after 5 days of storage and could not resist centrifugation stress unlike our emulsion stabilized with ELP-*g*-Bu. Looking at pH responsivity, the emulsion was destabilized at pH 4.5 and stable even after 3 cycles at pH 7, although the release of the dye was not studied[49]. Therefore, our ELP-*g*-Bu bioconjugate-stabilized emulsions seemed to combine storage and centrifugation stability and stimuli responsiveness. In another comparable study to some extent, a synthetic pH-responsive polymer based on PEI-benzaldehyde was evaluated for switchable O/W emulsion with paraffin oil processed by sonication. With synthetic polymer and ratio adjustment, the droplets were able to reach a nanometer size of 600-700 nm but remained stable only for 7 days. The demulsification with pH stimulus was only partial at pH 4.5 (but complete after 1 week) and rapidly occurred (within 5 minutes) at pH below 3.5. The emulsion was shown to be able to support emulsification and demulsification with pH adjustment back to 7.8 thanks to the dynamic covalent surfactant. Although a fluorescent dye was loaded in the emulsion, no release study was conducted to further compare both systems[43]. Overall, the ELP-*g*-Bu emulsions combined storage stability, responsiveness to thermal and ROS stimuli and proved to release loaded molecules. Thus, adding more value to the polypeptide-based smart polymer potential as the pH responsiveness of stabilized emulsion was previously demonstrated[50].

## 4. Conclusion

In this study, the potential of the amphiphilic ELP-*g*-Bu bioconjugate was investigated to stabilize conventional O/W emulsions and trigger the release of loaded molecules upon dual stimuli, namely temperature and oxidative conditions. To this aim, physico-chemical properties were first evaluated mainly by determining of the critical aggregation concentrations of ELP derivatives to evaluate the impact of parameters, namely temperature, the presence of salt, the presence of a positive charge in the ELP-*g*-Bu($S^+$), and thioether group oxidation with the control compound ELP-*g*-Bu(SO). Overall, all ELP derivatives showed surfactant properties, but only ELP-*g*-Bu CAC was strongly affected by oxidation. The amphiphilic ELP-*g*-Bu was subsequently evaluated for emulsion formulation regarding its thermal and oxidation responsive behaviors. The latter demonstrated its ability to stabilize oil-in-water emulsions with a weight ratio of 10:10:80 (ELP-*g*-Bu:Oil:Water) leading to droplets of a mean size of 9 ± 1 µm stable for at least a month at 4 and 25 °C. Lastly, the complete release of loaded fluorescent molecule from the emulsions was observed when the temperature was raised to 42°C, while a partial release was measured in oxidative conditions. An increase in oxidable thioether groups in such bioconjugate would likely lead to a higher shift in the HLB and better destabilization of the emulsions. Overall, ELP-*g*-Bu demonstrated its potential for smart polymer-based drug delivery systems that can be promising for inflammatory diseases treatment as increased temperature and ROS are present in such diseases[51].

## 5. Acknowledgement

Preliminary work from C. Feuilloley and V. Ibrahimova on similar ELP derivatives is acknowledged since useful for the present study. The authors would also like to thank Rania Ghamgui for her contribution to this work. We acknowledge the China Scholarship Council and Université de Bordeaux (UB-CSC 2021) for specific funding to D.Z. This work was funded by the European Union's Horizon Europe research and innovation program under the grant agreement No. 101079482 ("SUPRALIFE"). Continuous support from Univ. Bordeaux, CNRS and Bordeaux-INP is greatly acknowledged.

## 6. References


(1) Muschiolik, G. Multiple Emulsions for Food Use. *Curr Opin Colloid Interface Sci* **2007**, *12* (4–5), 213–220. https://doi.org/10.1016/j.cocis.2007.07.006.

(2) Marti-Mestres, G.; Nielloud, F. Emulsions in Health Care Applications—An Overview. *J Dispers Sci Technol* **2002**, *23* (1–3), 419–439. https://doi.org/10.1080/01932690208984214.

(3) Adams, F.; Kabalnov, A. S.; Petsev, D. N.; Obey, T.; Vincent, B.; Kunieda, H.; Pons, R.; Solans, C.; Forster, T. H.; Von Rybinski, W. *Modern Aspects of Emulsion Science*; Royal Society of Chemistry, 2007.

(4) Jeong, B.; Gutowska, A. Lessons from Nature: Stimuli-Responsive Polymers and Their Biomedical Applications. *Trends Biotechnol* **2002**, *20* (7), 305–311. https://doi.org/10.1016/S0167-7799(02)01962-5.

(5) Bharti, D.; Banerjee, I.; Sarkar, P.; Kim, D.; Pal, K. Smart Polymers for Biomedical Applications. In *Advances in Biomedical Polymers and Composites*; Elsevier, 2023; pp 223–246. https://doi.org/10.1016/B978-0-323-88524-9.00010-3.

(6) Fattah-alhosseini, A.; Chaharmahali, R.; Alizad, S.; Kaseem, M.; Dikici, B. A Review of Smart Polymeric Materials: Recent Developments and Prospects for Medicine Applications. *Hybrid Advances* **2024**, *5*, 100178. https://doi.org/10.1016/j.hybadv.2024.100178.

(7) Rajbanshi, A.; Hilton, E.; Dreiss, C. A.; Murnane, D.; Cook, M. T. Stimuli-Responsive Polymers for Engineered Emulsions. *Macromol Rapid Commun* **2024**, *45* (10). https://doi.org/10.1002/marc.202300723.

(8) Wu, Y.; Zeng, M.; Cheng, Q.; Huang, C. Recent Progress toward Physical Stimuli-Responsive Emulsions. *Macromol Rapid Commun* **2022**, *43* (18). https://doi.org/10.1002/marc.202200193.

(9) Ge, X.; Mo, L.; Yu, A.; Tian, C.; Wang, X.; Yang, C.; Qiu, T. Stimuli-Responsive Emulsions: Recent Advances and Potential Applications. *Chin J Chem Eng* **2022**, *41*, 193–209. https://doi.org/10.1016/j.cjche.2021.11.002.

(10) Wang, Z.; Jia, K.; Liu, T.; Hu, J.; Li, X.; Dong, J. PH and Light Reconfigured Complex Emulsions by Stimuli-Responsive Surfactants. *Acta Physico-Chimica Sinica* **2019**, *35* (1), 84–91. https://doi.org/10.3866/PKU.WHXB201712251.

(11) Roberts, S.; Costa, S.; Schaal, J.; Simon, J. R.; Dzuricky, M.; Quiroz, F. G.; Chilkoti, A. 2.5 Elastin-Like Polypeptides ☆. In *Comprehensive Biomaterials II*; Elsevier, 2017; pp 90–108. https://doi.org/10.1016/B978-0-12-803581-8.09308-5.

(12) Rodríguez-Cabello, J. C.; Martín, L.; Alonso, M.; Arias, F. J.; Testera, A. M. "Recombinamers" as Advanced Materials for the Post-Oil Age. *Polymer (Guildf)* **2009**, *50* (22), 5159–5169. https://doi.org/10.1016/j.polymer.2009.08.032.

(13) McPherson, D. T.; Xu, J.; Urry, D. W. Product Purification by Reversible Phase Transition FollowingEscherichia ColiExpression of Genes Encoding up to 251 Repeats of the Elastomeric Pentapeptide GVGVP. *Protein Expr Purif* **1996**, *7* (1), 51–57. https://doi.org/10.1006/prep.1996.0008.

(14) Meyer, D. E.; Chilkoti, A. A. *Molecular Cloning: A Laboratory Manual*, 4th edition.; 2002; Vol. Chapter 18.

(15) Meyer, D. E.; Chilkoti, A. Genetically Encoded Synthesis of Protein-Based Polymers with Precisely Specified Molecular Weight and Sequence by Recursive Directional Ligation: Examples from the

Elastin-like Polypeptide System. *Biomacromolecules* **2002**, *3* (2), 357–367. https://doi.org/10.1021/bm015630n.

(16) Chilkoti, A.; Chtistensen, T.; Mackay, J. Stimulus Responsive Elastin Biopolymers: Applications in Medicine and Biotechnology. *Curr Opin Chem Biol* **2006**, *10* (6), 652–657. https://doi.org/10.1016/j.cbpa.2006.10.010.

(17) MacEwan, S. R.; Chilkoti, A. Elastin-like Polypeptides: Biomedical Applications of Tunable Biopolymers. *Peptide Science* **2010**, *94* (1), 60–77. https://doi.org/10.1002/bip.21327.

(18) Varanko, A. K.; Su, J. C.; Chilkoti, A. Elastin-Like Polypeptides for Biomedical Applications. *Annu Rev Biomed Eng* **2020**, *22* (1), 343–369. https://doi.org/10.1146/annurev-bioeng-092419-061127.

(19) Despanie, J.; Dhandhukia, J. P.; Hamm-Alvarez, S. F.; MacKay, J. A. Elastin-like Polypeptides: Therapeutic Applications for an Emerging Class of Nanomedicines. *Journal of Controlled Release* **2016**, *240*, 93–108. https://doi.org/10.1016/j.jconrel.2015.11.010.

(20) Garanger, E.; MacEwan, S. R.; Sandre, O.; Brûlet, A.; Bataille, L.; Chilkoti, A.; Lecommandoux, S. Structural Evolution of a Stimulus-Responsive Diblock Polypeptide Micelle by Temperature Tunable Compaction of Its Core. *Macromolecules* **2015**, *48* (18), 6617–6627. https://doi.org/10.1021/acs.macromol.5b01371.

(21) Ibrahimova, V.; Zhao, H.; Ibarboure, E.; Garanger, E.; Lecommandoux, S. Thermosensitive Vesicles from Chemically Encoded Lipid-Grafted Elastin-like Polypeptides. *Angewandte Chemie International Edition* **2021**, *60* (27), 15036–15040. https://doi.org/10.1002/anie.202102807.

(22) Park, W. M.; Champion, J. A. Thermally Triggered Self-Assembly of Folded Proteins into Vesicles. *J Am Chem Soc* **2014**, *136* (52), 17906–17909. https://doi.org/10.1021/ja5090157.

(23) Dautel, D. R.; Heller, W. T.; Champion, J. A. Protein Vesicles with PH-Responsive Disassembly. *Biomacromolecules* **2022**, *23* (9), 3678–3687. https://doi.org/10.1021/acs.biomac.2c00562.

(24) Dreher, M. Evaluation of an Elastin-like Polypeptide–Doxorubicin Conjugate for Cancer Therapy. *Journal of Controlled Release* **2003**, *91* (1–2), 31–43. https://doi.org/10.1016/S0168-3659(03)00216-5.

(25) Bhattacharyya, J.; Bellucci, J. J.; Weitzhandler, I.; McDaniel, J. R.; Spasojevic, I.; Li, X.; Lin, C.-C.; Chi, J.-T. A.; Chilkoti, A. A Paclitaxel-Loaded Recombinant Polypeptide Nanoparticle Outperforms Abraxane in Multiple Murine Cancer Models. *Nat Commun* **2015**, *6* (1), 7939. https://doi.org/10.1038/ncomms8939.

(26) Dreher, M. R.; Simnick, A. J.; Fischer, K.; Smith, R. J.; Patel, A.; Schmidt, M.; Chilkoti, A. Temperature Triggered Self-Assembly of Polypeptides into Multivalent Spherical Micelles. *J Am Chem Soc* **2008**, *130* (2), 687–694. https://doi.org/10.1021/ja0764862.

(27) Weinberger, A.; Walter, V.; MacEwan, S. R.; Schmatko, T.; Muller, P.; Schroder, A. P.; Chilkoti, A.; Marques, C. M. Cargo Self-Assembly Rescues Affinity of Cell-Penetrating Peptides to Lipid Membranes. *Sci Rep* **2017**, *7* (1), 43963. https://doi.org/10.1038/srep43963.

(28) Hassouneh, W.; Fischer, K.; MacEwan, S. R.; Branscheid, R.; Fu, C. L.; Liu, R.; Schmidt, M.; Chilkoti, A. Unexpected Multivalent Display of Proteins by Temperature Triggered Self-Assembly of Elastin-like Polypeptide Block Copolymers. *Biomacromolecules* **2012**, *13* (5), 1598–1605. https://doi.org/10.1021/bm300321n.

(29) Dai, M.; Georgilis, E.; Goudounet, G.; Garbay, B.; Pille, J.; van Hest, J. C. M.; Schultze, X.; Garanger, E.; Lecommandoux, S. Refining the Design of Diblock Elastin-Like Polypeptides for Self-Assembly into Nanoparticles. *Polymers (Basel)* **2021**, *13* (9), 1470. https://doi.org/10.3390/polym13091470.

(30) Petitdemange, R.; Garanger, E.; Bataille, L.; Bathany, K.; Garbay, B.; Deming, T. J.; Lecommandoux, S. Tuning Thermoresponsive Properties of Cationic Elastin-like Polypeptides by Varying Counterions and Side-Chains. *Bioconjug Chem* **2017**, *28* (5), 1403–1412. https://doi.org/10.1021/acs.bioconjchem.7b00082.

(31) Rosselin, M.; Xiao, Y.; Belhomme, L.; Lecommandoux, S.; Garanger, E. Expanding the Toolbox of Chemoselective Modifications of Protein-Like Polymers at Methionine Residues. *ACS Macro Lett* **2019**, *8* (12), 1648–1653. https://doi.org/10.1021/acsmacrolett.9b00862.

(32) Anaya, L. M. B.; Petitdemange, R.; Rosselin, M.; Ibarboure, E.; Garbay, B.; Garanger, E.; Deming, T. J.; Lecommandoux, S. Design of Thermoresponsive Elastin-Like Glycopolypeptides for Selective Lectin Binding and Sorting. *Biomacromolecules* **2021**, *22* (1), 76–85. https://doi.org/10.1021/acs.biomac.0c00374.

(33) Rosselin, M.; Chinoy, Z. S.; Bravo-Anaya, L. M.; Lecommandoux, S.; Garanger, E. Multivalent Elastin-Like Glycopolypeptides: Subtle Chemical Structure Modifications with High Impact on Lectin Binding Affinity. *ACS Macro Lett* **2021**, *10* (1), 65–70. https://doi.org/10.1021/acsmacrolett.0c00775.

(34) Bravo-Anaya, L. M.; Garbay, B.; Nando-Rodríguez, J. L. E.; Carvajal Ramos, F.; Ibarboure, E.; Bathany, K.; Xia, Y.; Rosselgong, J.; Joucla, G.; Garanger, E.; Lecommandoux, S. Nucleic Acids Complexation with Cationic Elastin-like Polypeptides: Stoichiometry and Stability of Nano-Assemblies. *J Colloid Interface Sci* **2019**, *557*, 777–792. https://doi.org/10.1016/j.jcis.2019.09.054.

(35) Bravo-Anaya, L. M.; Rosselgong, J.; Fernández-Solís, K. G.; Xiao, Y.; Vax, A.; Ibarboure, E.; Ruban, A.; Lebleu, C.; Joucla, G.; Garbay, B.; Garanger, E.; Lecommandoux, S. Coupling of RAFT Polymerization and Chemoselective Post-Modifications of Elastin-like Polypeptides for the Synthesis of Gene Delivery Hybrid Vectors. *Polym Chem* **2021**, *12* (2), 226–241. https://doi.org/10.1039/D0PY01293A.

(36) Petitdemange, R.; Garanger, E.; Bataille, L.; Dieryck, W.; Bathany, K.; Garbay, B.; Deming, T. J.; Lecommandoux, S. Selective Tuning of Elastin-like Polypeptide Properties via Methionine Oxidation. *Biomacromolecules* **2017**, *18* (2), 544–550. https://doi.org/10.1021/acs.biomac.6b01696.

(37) Ibrahimova, V.; González-Delgado, J. A.; Levêque, M.; Torres, T.; Garanger, E.; Lecommandoux, S. Photooxidation Responsive Elastin-Like Polypeptide Conjugates for Photodynamic Therapy Application. *Bioconjug Chem* **2021**, *32* (8), 1719–1728. https://doi.org/10.1021/acs.bioconjchem.1c00251.

(38) Otulakowski, Ł.; Kasprów, M.; Strzelecka, A.; Dworak, A.; Trzebicka, B. Thermal Behaviour of Common Thermoresponsive Polymers in Phosphate Buffer and in Its Salt Solutions. *Polymers (Basel)* **2020**, *13* (1), 90. https://doi.org/10.3390/polym13010090.

(39) Christensen, T.; Hassouneh, W.; Trabbic-Carlson, K.; Chilkoti, A. Predicting Transition Temperatures of Elastin-Like Polypeptide Fusion Proteins. *Biomacromolecules* **2013**, *14* (5), 1514–1519. https://doi.org/10.1021/bm400167h.

(40) Cho, Y.; Zhang, Y.; Christensen, T.; Sagle, L. B.; Chilkoti, A.; Cremer, P. S. Effects of Hofmeister Anions on the Phase Transition Temperature of Elastin-like Polypeptides. *J Phys Chem B* **2008**, *112* (44), 13765–13771. https://doi.org/10.1021/jp8062977.

(41) Sadeghi, R.; Jahani, F. Salting-In and Salting-Out of Water-Soluble Polymers in Aqueous Salt Solutions. *J Phys Chem B* **2012**, *116* (17), 5234–5241. https://doi.org/10.1021/jp300665b.

(42) Feng, H.; Verstappen, N. A. L.; Kuehne, A. J. C.; Sprakel, J. Well-Defined Temperature-Sensitive Surfactants for Controlled Emulsion Coalescence. *Polym Chem* **2013**, *4* (6), 1842. https://doi.org/10.1039/c2py21007j.

(43) Ren, G.; Wang, L.; Chen, Q.; Xu, Z.; Xu, J.; Sun, D. PH Switchable Emulsions Based on Dynamic Covalent Surfactants. *Langmuir* **2017**, *33* (12), 3040–3046. https://doi.org/10.1021/acs.langmuir.6b04546.

(44) Pei, X.; Zhang, S.; Zhang, W.; Liu, P.; Song, B.; Jiang, J.; Cui, Z.; Binks, B. P. Behavior of Smart Surfactants in Stabilizing PH-Responsive Emulsions. *Angewandte Chemie International Edition* **2021**, *60* (10), 5235–5239. https://doi.org/10.1002/anie.202013443.

(45) Li, X.; Zhu, P.; Lv, X.; Yan, G.; Lu, H. Redox and Doubly PH-Switchable Pickering Emulsion. *Langmuir* **2020**, *36* (47), 14288–14295. https://doi.org/10.1021/acs.langmuir.0c02505.

(46) Verbrugghe, S.; Bernaerts, K.; Du Prez, F. E. Thermo-Responsive and Emulsifying Properties of Poly( *N* -vinylcaprolactam) Based Graft Copolymers. *Macromol Chem Phys* **2003**, *204* (9), 1217–1225. https://doi.org/10.1002/macp.200390098.

(47) Koh, A. Y. C.; Saunders, B. R. Thermally Induced Gelation of an Oil-in-Water Emulsion Stabilised by a Graft Copolymer. *Chemical Communications* **2000**, No. 24, 2461–2462. https://doi.org/10.1039/b008334h.

(48) Alava, C.; Saunders, B. R. Effect of Added Surfactant on Temperature-Induced Gelation of Emulsions. *Langmuir* **2004**, *20* (8), 3107–3113. https://doi.org/10.1021/la036371l.

(49) Tirgarian, B.; Farmani, J.; Farahmandfar, R.; Milani, J. M.; Van Bockstaele, F. Switchable PH-Responsive Biopolymeric Stabilizers Made by Sonothermal Glycation of Sodium Caseinate with Kappa-Carrageenan. *Food Biophys* **2023**, *18* (3), 362–378. https://doi.org/10.1007/s11483-023-09778-7.

(50) Lecommandoux, S.; Dupin, D.; Loinaz Bordonabe, I.; Grande Telleria, H. New Polymeric Emulsifier and Uses Thereof for the Encapsulation of Hydrophobic or Hydrophilic Active Compounds. WO/2019/068936, 2019.

(51) Medzhitov, R. Origin and Physiological Roles of Inflammation. *Nature* **2008**, *454* (7203), 428–435. https://doi.org/10.1038/nature07201.

# Dual responsive emulsions based on amphiphilic elastin-like polypeptide bioconjugates

*Laurianne Simon,[1,Π*] Dongxu Zhou,[2,Π] Anita Coeurvolan,[1] Vincent Lapinte,[1] Sébastien Lecommandoux,[2] Elisabeth Garanger,[2,*] and Sylvie Bégu[1,*]*

[1] ICGM, Univ. Montpellier, CNRS, ENSCM, Montpellier, France
[2] Université de Bordeaux, CNRS, Bordeaux INP, LCPO, UMR 5629, ENSMAC, 16 avenue Pey-Berland, Pessac F-33600, France

Π co-first authors

Laurianne.simon@umontpellier.fr
Elisabeth.garanger@u-bordeaux.fr
Sylvie.begu@umontpellier.fr

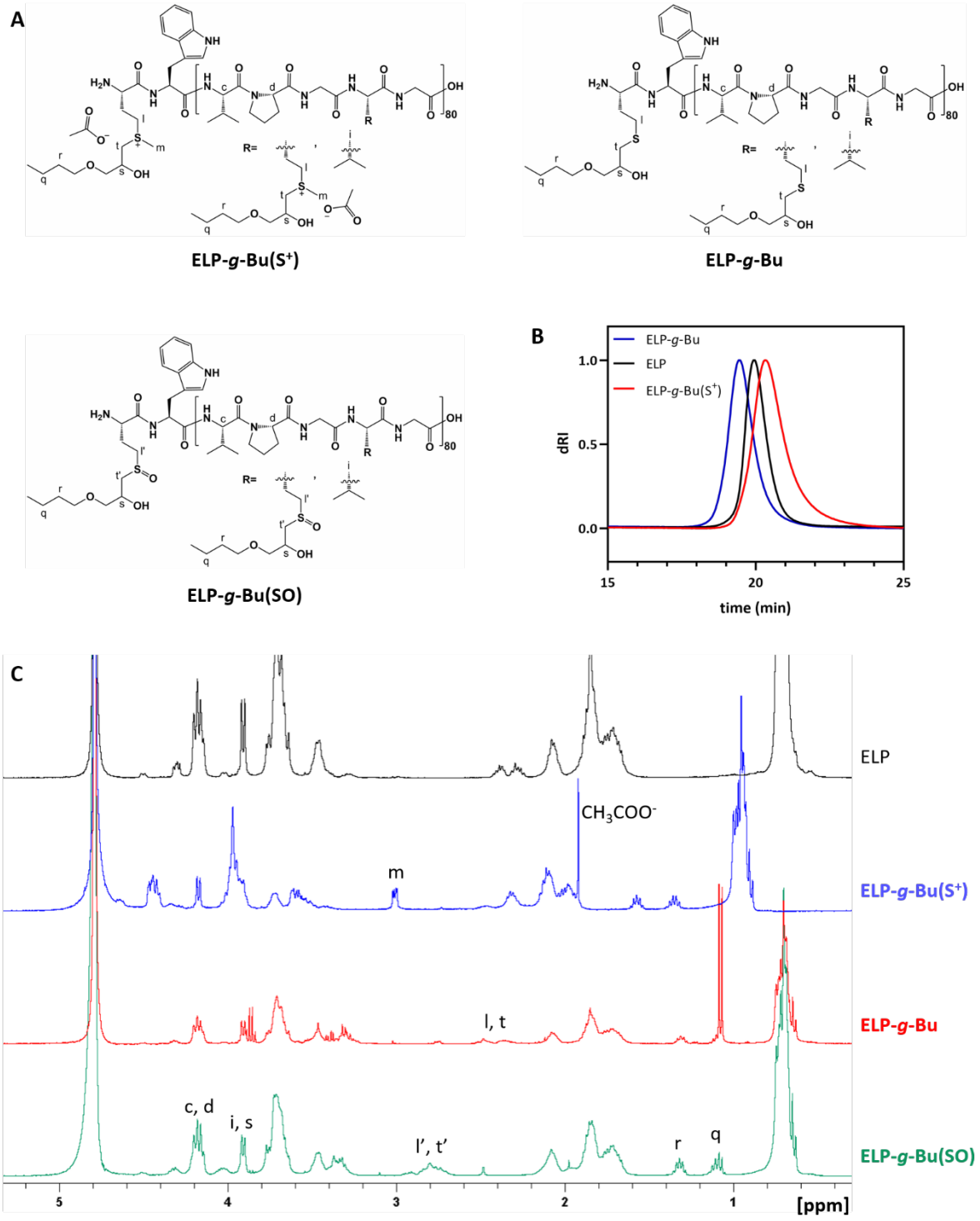


Figure S1. Chemical structures of ELP-*g*-Bu($S^+$), ELP-*g*-Bu and ELP-*g*-Bu(SO). B) Characterization of ELP, ELP-*g*-Bu($S^+$) and ELP-*g*-Bu by SEC in DMSO. C) $^1$H NMR spectra of ELP, ELP-*g*-Bu($S^+$), ELP-*g*-Bu and ELP-*g*-Bu(SO) in $D_2O$.

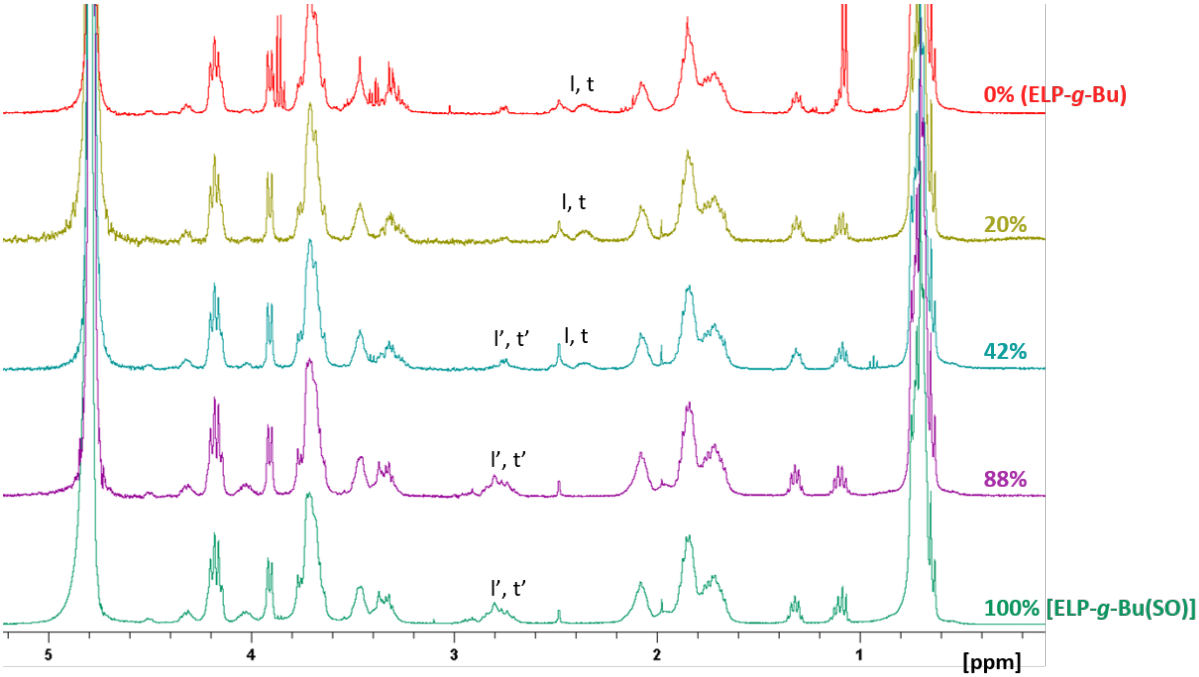


Figure S2. $^{1}$H NMR monitoring of ELP-*g*-Bu oxidation degree from 0 to 100 % to obtain ELP-*g*-Bu(SO).

Table S1. Calculation of oxidation degrees tracked by $^{1}$H NMR and the relation between the oxidation degree and the amount of $H_2O_2$ used.

| mol ($H_2O_2$)/ mmol (ELP-*g*-Bu) | AUC *l, t* | AUC *l', t'* | Ratio *l', t'*/82 | Degree of oxidation (%) |
|---|---|---|---|---|
| 0 | 83.50 | / | / | 0 |
| 0.21 | 65.80 | 16.59 | 0.202 | 20 |
| 1.06 | 48.58 | 34.64 | 0.422 | 42 |
| 42.56 | 9.79 | 71.83 | 0.876 | 88 |
| 63.84 | / | 82.45 | 1.005 | 100 |

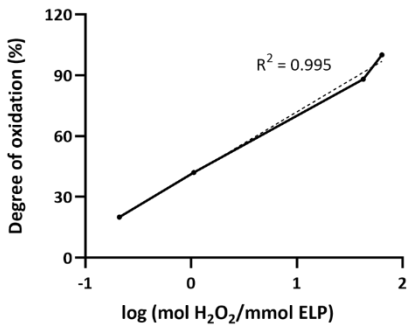

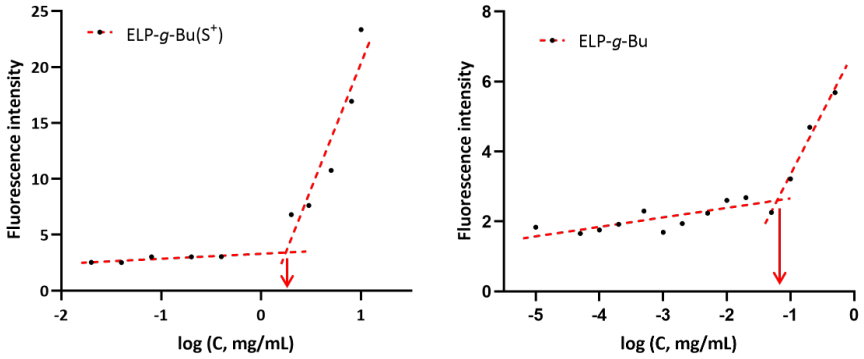


Figure S3. Determination of the CAC values of ELP-*g*-Bu($S^+$) and ELP-*g*-Bu in $H_2O$ using Nile red as fluorescent probe at 22 °C.

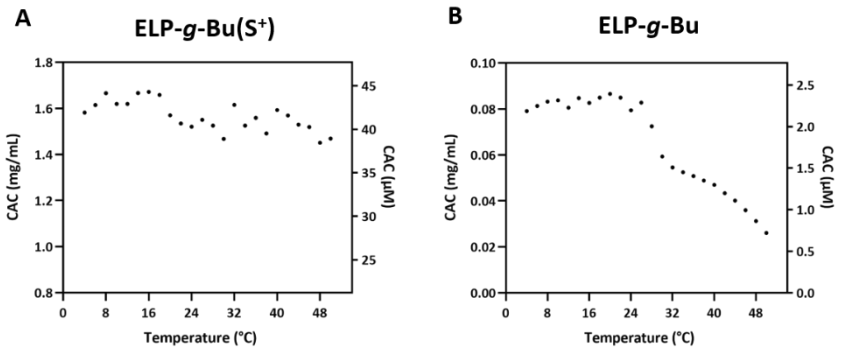


C

| At 22 °C | PBS | |
|---|---|---|
| | CAC (mg/mL) | CAC (μM) |
| **ELP-*g*-Bu($S^+$)** | 1.53 | 40.65 |
| **ELP-*g*-Bu** | 0.085 | 2.35 |

Figure S4. Determination of the critical aggregation concentration (CAC) in mass concentration (mg/mL) and molar concentration (μM) using Nile red as fluorescent probe in PBS upon temperature of A) ELP-*g*-Bu($S^+$) and B) ELP-*g*-Bu and C) the summary of CAC values at 22 °C for the two ELP derivatives in PBS.

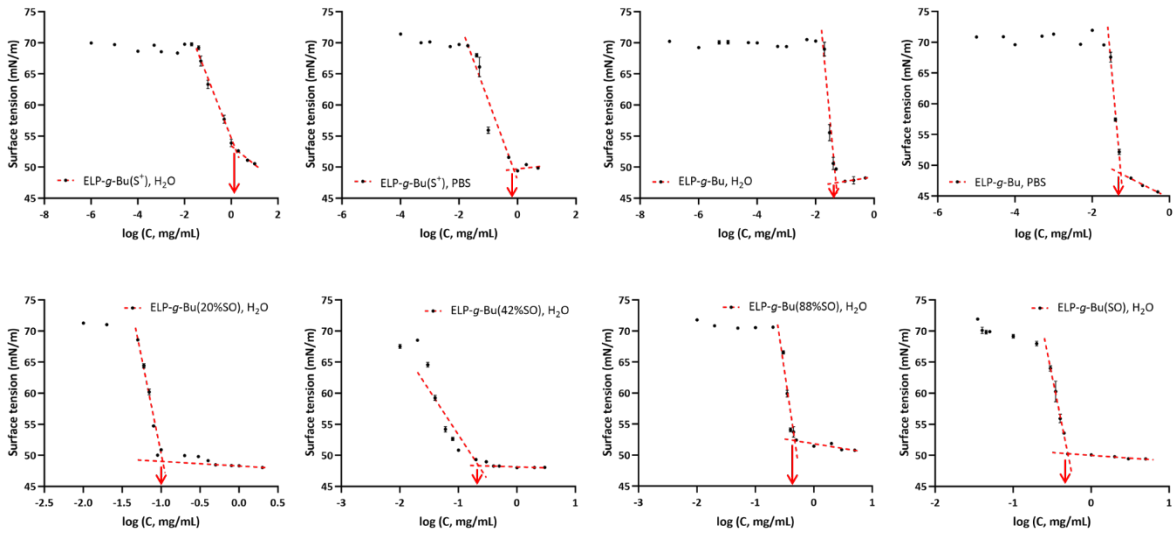


Figure S5. Determination of the CAC values of the different ELP derivatives in $H_2O$ or PBS by the pendant drop method at 22 °C.

Table S2. CAC results of ELP-*g*-Bu($S^+$) and ELP- *g*-Bu using the pendent drop method in water and in PBS at 22 °C.

| **Polymer** | **ELP-*g*-Bu($S^+$)** | | **ELP-*g*-Bu** | |
|---|---|---|---|---|
| Media | Water | PBS | Water | PBS |
| CAC (mg/mL) | 1.5 | 1.03 | 0.049 | 0.055 |
| CAC (µM) | 40.9 | 27.3 | 1.4 | 1.5 |
| Δ ST (mN/m) | 19.4 | 21.0 | 22.5 | 25.2 |

Table S3. CAC results of oxidized ELP-*g*-Bu from 20 % to 100 % (ELP-*g*-Bu(SO))with pendant drop method in water at 22 °C.

| **ELP-*g*-Bu(SO)** | **20%** | **42%** | **88%** | **100%** |
|---|---|---|---|---|
| CAC (mg/mL) | 0.10 | 0.22 | 0.49 | 0.50 |
| CAC (µM) | 2.9 | 6.1 | 13.5 | 13.7 |
| Δ ST (mN/m) | 23.2 | 20.5 | 20.9 | 22.5 |

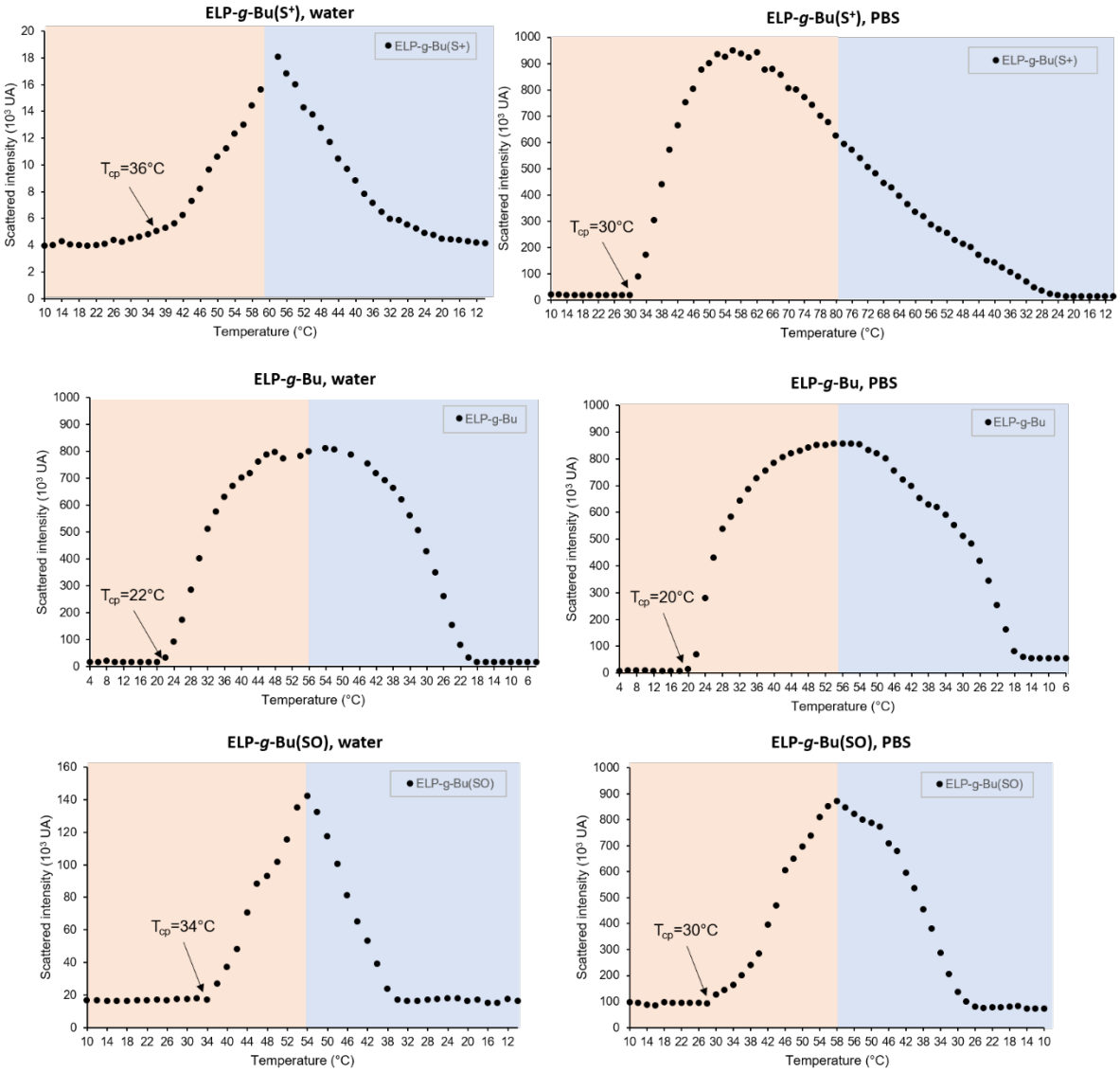


Figure S6. Determination of cloud temperature by nephelometry at 17 µM in water and in PBS for ELP-*g*-Bu($S^+$), ELP-*g*-Bu and ELP-*g*-Bu(SO).

Figure S7. Picture of ELP-*g*-Bu emulsion with a volume of 100 µL prepared in a glass vial of 4 mL.

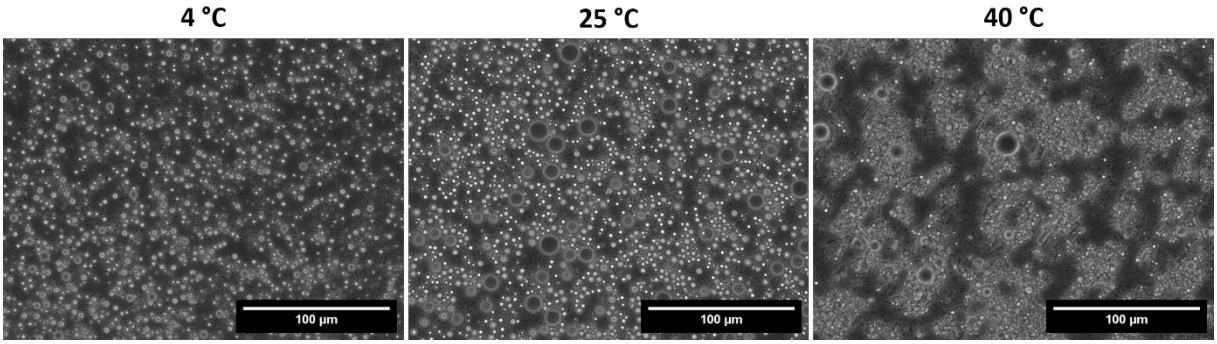


Figure S8. Observation of ELP-*g*-Bu emulsion after 28 days at 4°C and 25°C and tested for aggregation at 40°C under optical microscope EVOS life (x40).